ISIJ International, Vol. 52 (2012), No. 6, pp. 1124–1129

Microstructure and Retained Austenite Characteristics of Ultra High-strength TRIP-aided Martensitic Steels

Junya KOBAYASHI,[1] Sung-Moo SONG[2] and Koh-ichi SUGIMOTO[2]

1) Graduate Student, Shinshu University, 4-17-1, Wakasato, Nagano, 380-8553 Japan. E-mail: koba@sugimotolab.shinshu-u.ac.jp 2) Department of Mechanical Systems Engineering, Shinshu University, 4-17-1, Wakasato, Nagano, 380-8553 Japan. E-mail: song001@shinshu-u.ac.jp, sugimot@shinshu-u.ac.jp

(*Received on October 11, 2011; accepted on January 4, 2012*)

A new type of 0.2%C–1.5%Si–1.5%Mn ultra high-strength low alloy TRIP-aided steel consisting of lath martensite structure matrix and metastable retained austenite films, "TRIP-aided martensitic steel; TM steel", was developed by means of quenching and partitioning process. In addition, effects of partitioning temperature and time on the microstructure and retained austenite characteristics were investigated. The matrix structure was composed of two kinds of lath martensite structures, or wide and narrow lath martensite structures. Most of the retained austenite of about 3 vol% was located along the narrow martensite lath boundary. On the other hand, a small amount of fine and needle-like carbides precipitated only in wider lath martensite structure. Partitioning at temperatures lower than 250°C for 1 000 s after quenching in oil or ice brine considerably increased carbon concentration of the retained austenite phase to about 1.0 mass%, maintaining volume fractions of retained austenite and carbide. Also, the carbon-enrichment mechanism in the retained austenite was proposed through TEM observation, as well as the carbide precipitation and coarsening mechanisms.

KEY WORDS: ultra high-strength steel; TRIP-aided steel; retained austenite; microstructure; martensite; partitioning.

1. Introduction

In the past two or three decades, many advanced high-strength sheet steels for automobile parts have been developed to reduce the body weight of automobiles. According to De Cooman,[1] first-generation advanced high-strength steels (AHSSs), such as dual-phase steel, *Transformation-Induced Plasticity-aided steel* (TRIP-aided steel) with a polygonal ferrite matrix, and so on, have contributed considerably to the weight reduction and crash safety of recent automobiles because of their good combination of formability and tensile strength. Although second-generation AHSSs such as *Twinning-Induced Plasticity steel* (TWIP steel)[2] have not been applied so widely to automotive parts, third-generation advanced AHSSs such as *TRIP-aided bainitic ferrite steel* (TBF steel)[3–9] and *quenching and partitioning steel* (Q&P steel),[10] with good formability (stretch-flangeability and bendability) and ultra-high strength (980–1 470 MPa) are expected for future automotive applications. For the achievement of a tensile strength of more than 2.0 GPa, quenching-partitioning-tempering (Q–P–T) steel with a martensite matrix was developed by Wang *et al.*[11] They reported that ultra-high-strength TRIP-aided steel can be developed through the utilization of the martensite structure.

Further ultra-high strength may be achieved by changing the matrix structure into martensite with carbon-enriched metastable retained austenite. However, such a "*TRIP-aided martensitic steel* (*TM steel*)" has not yet been developed. Moreover, there have been no reports on the microstructural formation mechanism and carbon-enrichment mechanism of retained austenite in martensitic steels such as TM steel. In this study, TM steel with a chemical composition of 0.2% C, 1.5% Si, and 1.5% Mn (in mass%) is developed by means of quenching (to temperatures lower than M_f) and partitioning processes. In addition, the microstructural formation mechanisms and retained austenite characteristics are investigated.

2. Experimental Procedure

In this study, a 100-kg steel ingot was prepared by vacuum melting followed by hot forging to produce a bar of 32 mm in diameter. Then, the bars were heated to 1 200°C and hot-rolled to 13 mm in diameter with a finishing rolling temperature of 850°C, and cooled in air to room temperature. The chemical composition is detailed in **Table 1**. The measured CCT diagram is shown in **Fig. 1**, indicating a martensite start temperature M_S of about 420°C. In addition, the martensite finish temperature M_f is estimated to be 277°C.[9]

The heat-treatment diagram of TM steel is shown in **Fig.**

Table 1. Chemical composition (mass%) of a steel used.

C	Si	Mn	P	S	Al	N	O
0.20	1.50	1.50	0.015	0.0008	0.041	0.0005	0.0008

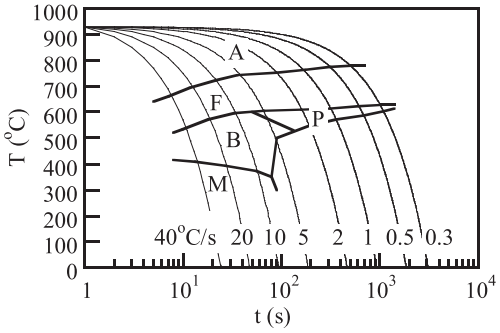

Fig. 1. Measured CCT diagram of steel used, in which A, F, P, B and M represent austenite, ferrite, pearlite, bainite and martensite, respectively.

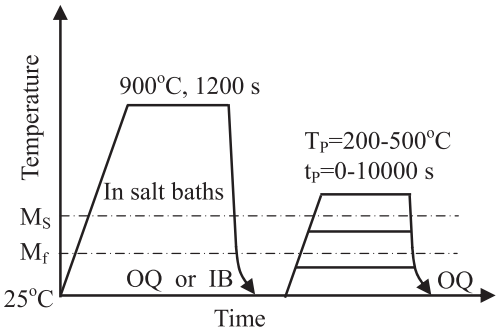

Fig. 2. Heat treatment diagram for TM steel, in which OQ and IB represent quenching in oil and ice-brine, respectively.

2. TM steel was partitioned at 200–500°C after quenching to room temperature in oil or ice-brine.

The retained austenite characteristics of the steel were investigated by X-ray diffractometry. Specimens were electropolished after grinding with Emery paper (#1 200). The volume fraction of retained austenite (f_γ, vol%) was quantified from the integrated intensity of the (200)α, (211)α, (200)γ, (220)γ, and (311)γ peaks obtained by X-ray diffractometry using Mo-Kα radiation.[12] The carbon concentration (C_γ, mass%) was estimated from the equation below. In this case, the lattice constant (a_γ, × 0.1 nm) was measured from the (200)γ, (220)γ, and (311)γ peaks of Cu-Kα radiation.[13]

$$a_\gamma = 3.5780 + 0.0330C_\gamma + 0.00095Mn_\gamma + 0.0056Al_\gamma + 0.0220N_\gamma \quad \text{..... (1)}$$

where Mn_γ, Al_γ, and N_γ represent the concentrations of the respective individual elements (mass%) in the retained austenite. For convenience, the contents of added alloying elements were substituted for these concentrations in this study.

The microstructure was observed by field-emission scanning electron microscopy (FE-SEM) with electron backscatter diffraction pattern (EBSP) equipment and transmission electron microscopy (TEM). Specimens for FE-SEM-EBSP analysis were ground with colloidal silica after grinding with alumina. The volume fraction of the carbide precipitation was measured through carbon extraction replicas.

Vickers hardness tests were carried out using a Vickers microhardness machine at 25°C, with a load of 0.98 N. The surface of the specimen was polished with Emery paper (#600).

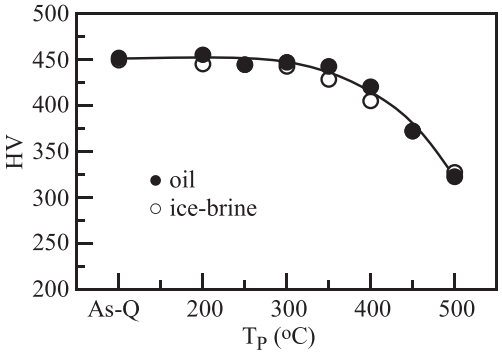

Fig. 3. Variations in Vickers hardness of TM steel as a function of partitioning temperature (T_P). Partitioning time (t_P) = 1 000 s.

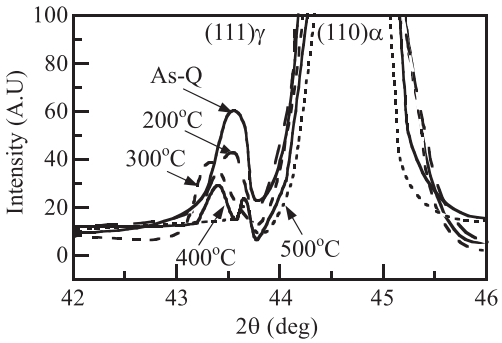

Fig. 4. Typical changes in X-ray diffraction patterns in TM steels as-quenched (As-Q) and partitioned at 200–500°C for 1 000 s after oil quenching.

3. Results

3.1. Vickers Hardness

Figure 3 shows the Vickers hardnesses of the TM steels. The TM steels subjected to quenching in oil and ice-brine have Vickers hardnesses of about HV450 at partitioning temperatures in the range 25–350°C. When the TM steels are partitioned at temperatures above 400°C, the Vickers hardness decreases with decreasing partitioning temperature.

3.2. Retained Austenite Characteristics

Figure 4 shows the typical change in the X-ray diffraction pattern of the retained austenite with partitioning temperature in the TM steel quenched in oil. **Figures 5** and **6** show the variations in the initial volume fraction and carbon concentration of the retained austenite of TM steels quenched in oil or ice-brine as a function of partitioning time and temperature, respectively. The TM steel quenched in oil contains retained austenite of a maximum of about 3 vol%. This amount decreases with increasing partitioning time in the range 100–10 000 s (Fig. 5) and with increasing partitioning temperature in the range 250–450°C (Fig. 6). On the other hand, the carbon concentration of the retained austenite increases considerably with increasing partitioning temperature and time. If the TM steel is quenched in ice-brine, the amount of retained austenite and its carbon concentration are reduced to about 1.6 vol% and 0.3 mass%, respectively.

3.3. Microstructure and Carbide

Figure 7 shows typical SEM images of the TM steel quenched in oil. **Figure 8** shows typical FE-SEM-EBSP analysis results for TM steel, and **Fig. 9** shows typical TEM images. From Figs. 7 and 8, the matrix structure of the present TM steel is found to consist of wide and narrow lath martensite structures, and hardly seems to change with partitioning temperature. It is also found that the wider lath martensite structure in TM steel gives a higher image quality than the narrower lath martensite structure, which means that the narrow lath martensite structure possesses a higher dislocation density.[14] It is noteworthy that there is no twin in the narrow lath martensite, or the narrow martensite is α'-martensite and not ε-martensite. As shown in Figs. 8(d),

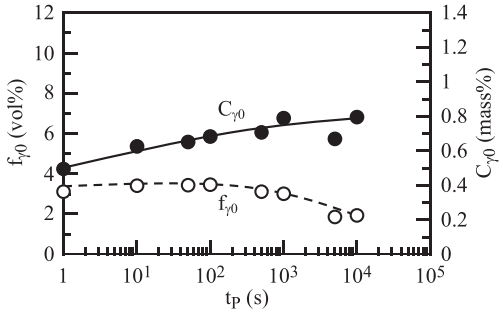

Fig. 5. Variations in initial volume fraction ($f_{\gamma 0}$) and initial carbon concentration ($C_{\gamma 0}$) of retained austenite as a function of partitioning time (t_P) in TM steel (quenching in oil). T_P = 250°C.

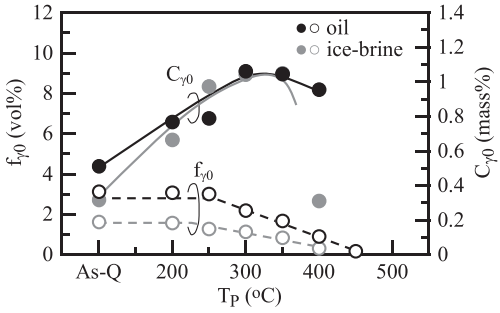

Fig. 6. Variations in initial volume fraction ($f_{\gamma 0}$) and initial carbon concentration ($C_{\gamma 0}$) of retained austenite as a function of partitioning temperature (T_P) in TM steel. t_P = 1 000 s.

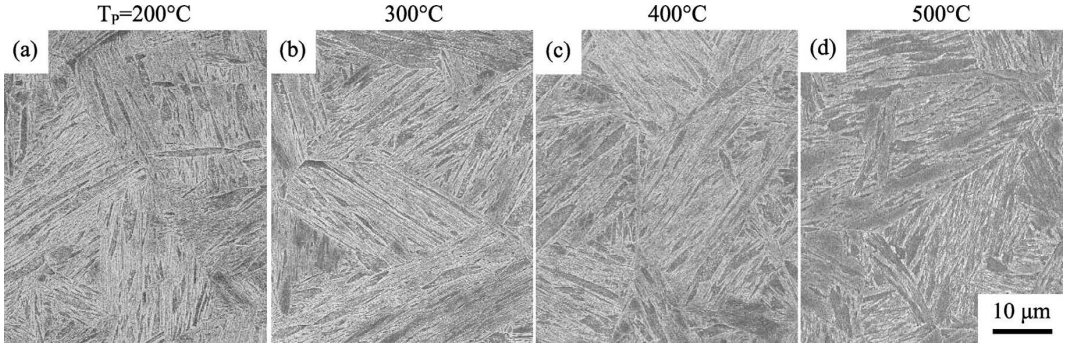

Fig. 7. Typical SEM images of TM steel subjected to partitioning process at (a) 200°C, (b) 300°C, (c) 400°C or (d) 500°C for 1 000 s.

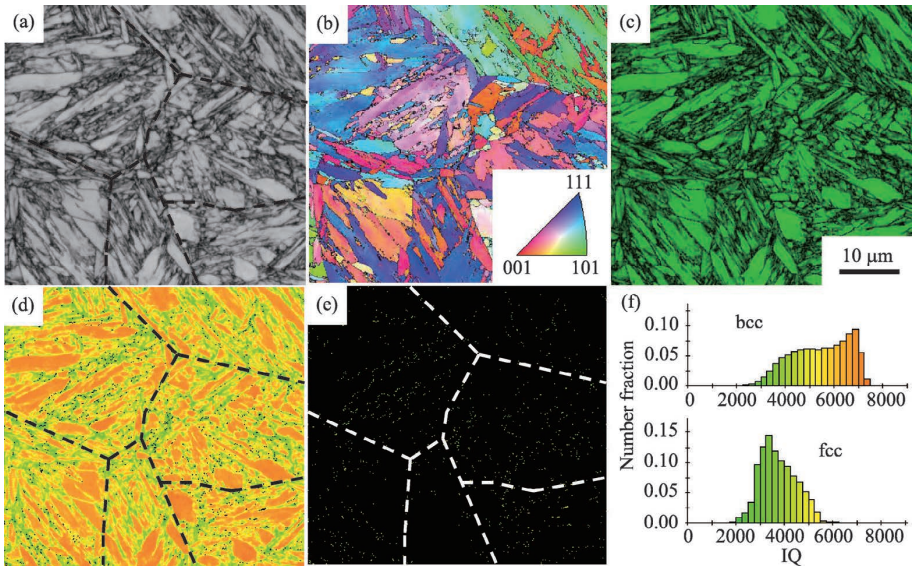

Fig. 8. (a) Image quality map, (b) inverse pole figure map, (c) phase map, (d) image quality distribution map of bcc phase, (e) image quality distribution map of fcc phase and (f) number fraction of image quality (IQ) of bcc and fcc phases in TM steel partitioned at 250°C for 1 000 s. In (c), green and red phases denote matrix structure (bcc) and retained austenite (fcc), respectively. In (d), darker yellow and yellowish green regions represent martensite lath structures with higher and lower image quality index, respectively. Black phases are other ones such as retained austenite phases. Dotted lines in (a), (d) and (e) represent prior austenitic grain boundary.

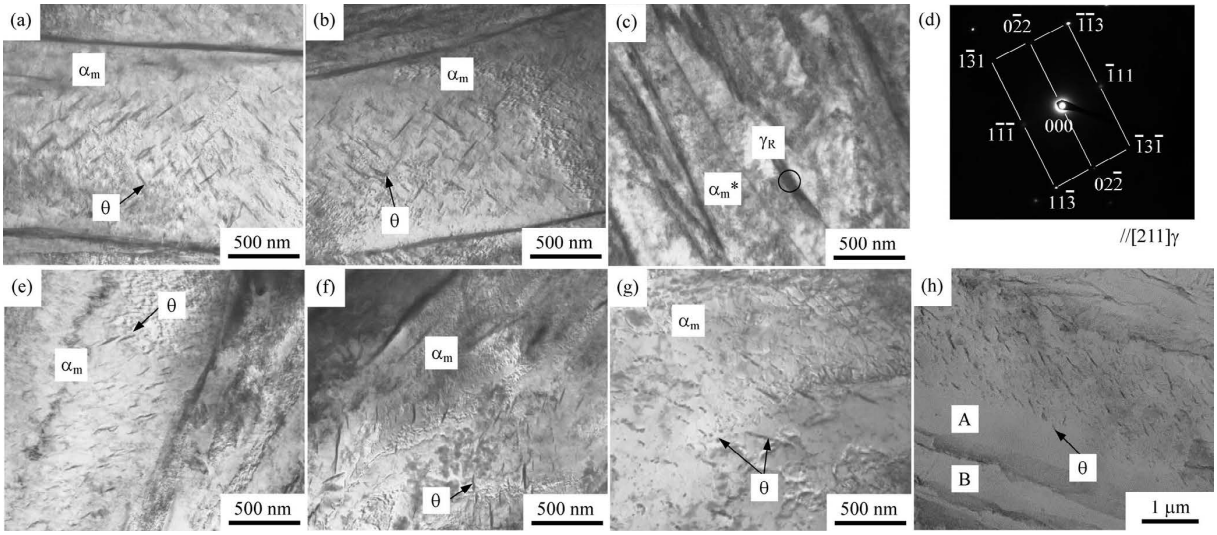

Fig. 9. TEM images of lath martensite structure in TM steel subjected to partitioning at (a) 25°C (as quenched), (b-d, h) 200°C, (e) 300°C, (f) 400°C or (g) 500°C for 1 000 s. (a), (b), (e), (f) and (g): wide lath martensite structure (α_m) with carbides (θ). (c): narrow lath martensite structure (α_m*) and interlath retained austenite (γ_R), (d): selected area diffraction pattern of circle in (c). (h): carbides observed by extraction replicas, in which A and B represent wide lath martensite structure with carbides (f_θ = 1.7 vol%) and narrow lath martensite structure without carbides, respectively.

8(e), and 9(c), most of the retained austenite phases are fine, and are located on the interlath boundary of the narrow martensite lath structure, which is yellowish green in Fig. 8(d).

In Figs. 9(a), 9(b), and 9(e)–9(h), a large amount of fine and needle-shaped carbide seems to precipitate only in the wider martensite lath structure. This means that the needle-shaped carbides are already precipitated through auto-tempering upon quenching. According to De Cooman and Speer,[1)] the martensite structure in Q&P steel includes transition ε- or η-carbide. In this study, some carbides were observed in the TM steel (Fig. 9), but the precipitates were not detected as ε- or η-carbide, so the carbides are considered as cementites.

The volume fraction of carbide in the present TM steel was too low to be measured by X-Ray diffractometry (Fig. 4). Therefore, in order to measure the carbide volume fraction accurately, we observed it through carbon extraction replicas for TM steels partitioned at 25–500°C. As an example, a typical TEM image of the extraction replicas is shown in Fig. 9(h). The measured volume fraction of carbide is shown in **Fig. 10**. The amount of carbide in the TM steel hardly changes when it is partitioned at temperatures below 250°C (f_θ = 1.7–2.0 vol%). The carbide fraction appears to increase with increasing partitioning temperature at temperatures above 250°C, accompanied by coarsening of the carbide. In the partitioning range above 450°C, the amount of carbide increases further (f_θ = 5.2 vol%). The carbide fraction of the TM steel quenched in ice-brine and then partitioned at 200°C (f_θ = 1.2 vol%) is lower than that of TM steel quenched in oil. Note that the amount of carbide in TM steel partitioned at 300°C for 1 000 s is considerably lower than that (f_θ = 5.7 vol%) of SCM420 steel (0.21%C–0.21%Si–0.77%Mn–1.02%Cr–0.18%Mo–0.06%Ni, in mass%) quenched in oil and then tempered at 300°C for 3 600 s.

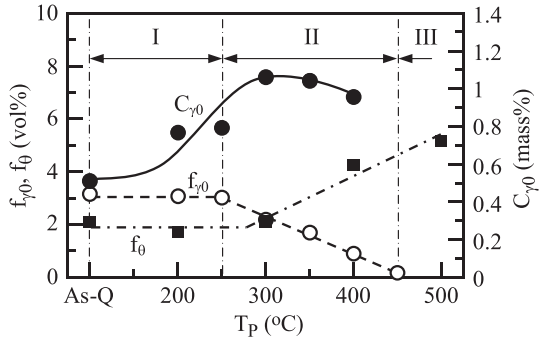

Fig. 10. Variations in volume fraction of carbide (f_θ: ■) and volume fraction ($f_{\gamma 0}$: ○) and carbon concentration ($C_{\gamma 0}$: ●) of retained austenite as a function of partitioning temperature (T_P) of TM steel quenched in oil.

4. Discussion

Figures 7–9 showed that TM steel subjected to the quenching and partitioning process consists of a wide and narrow lath martensite structure matrix and retained austenite located along the narrow martensite lath boundary, with precipitation of a small amount of carbide in the wide lath martensite structure. In general, Si suppresses carbide formation in steel,[5,15)] similarly to Al.[9)] Thus, it is considered that Si addition of 1.5 mass% results in such microstructural characteristics. In this case, a high shearing stress or free energy is required in the retained austenite for martensite transformation, because most of the retained austenite films are fine and surrounded by a hard martensite lath structure.

In the following, the transformation and carbide precipitation behavior of such a microstructure during the quenching and partitioning processes is discussed.

4.1. Microstructural Change on Quenching

The microstructural change and the retained austenite

characteristics during the quenching process are illustrated in **Fig. 11**. On quenching, the austenite is transformed into two kinds of lath martensite structure matrices. The transformation behavior can be summarized as follows.

Stages 1–3: When the steel is cooled to temperatures below M_S after heating in the γ region, the wide martensite structure is first formed preferentially (stages 1–2 in Fig. 11(c)). Carbides are not yet precipitated in the wide martensite structure.

Stages 3–4: On continuous cooling to room temperature below M_f, the untransformed austenite is transformed to the narrow martensite structure and retained as retained austenite (stages 3–4 in Fig. 11(c)). At the same time, the wide martensite structure is tempered through auto-tempering, and therefore, carbide is precipitated only in the wider martensite lath structure because of carbon diffusion.

According to Koistinen and Marburger,[16] the amount of martensite structure ($f\alpha_m$) increases with decreasing isothermal transformation temperature (T_{IT}) in conventional structural steel as follows:

$$f\alpha_m = 1 - \exp\{-A(M_S - T_{IT})^B\} \quad \text{..... (2)}$$

where A and B are material constants. If the present steel is subjected to the isothermal transformation process at temperatures between M_f and room temperature, the volume fractions of narrow martensite and retained austenite may increase. In fact, the above forecast was verified by Kobayashi *et al.*[17] with an investigation of the mechanical properties of TM steel.

In Fig. 6, it is seen that the volume fraction and carbon concentration of the retained austenite decrease more with decreasing carbide content when the TM steel is quenched in ice-brine than when it is quenched in oil. This is because of the increasing volume fraction of martensite due to the lower quenching temperature in ice-brine. It may also be associated with the shorter diffusion time that results from rapid quenching.

4.2. Carbon-enrichment Mechanism during Partitioning

The microstructural changes in the behavior of this TM steel during the partitioning process (stages 5–6 in Fig. 11(c)) at temperatures between 200 and 500°C are illustrated in **Fig. 12**, and are classified into three partitioning rang-

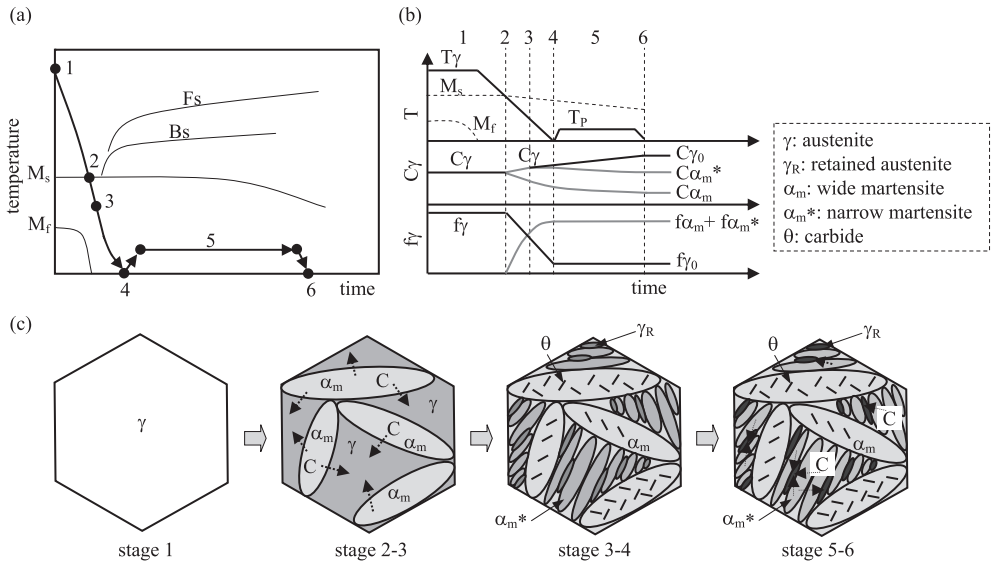

Fig. 11. Illustrations of (a) heat treatment diagram, (b) changes in carbon concentrations (C_γ, $C\alpha_m$ and $C\alpha_m$*) and volume fractions (f_γ, $f\alpha_m$ and $f\alpha_m$*) and (c) microstructural change at stages 1 through 6 of TM steel during partitioning process at 200°C.

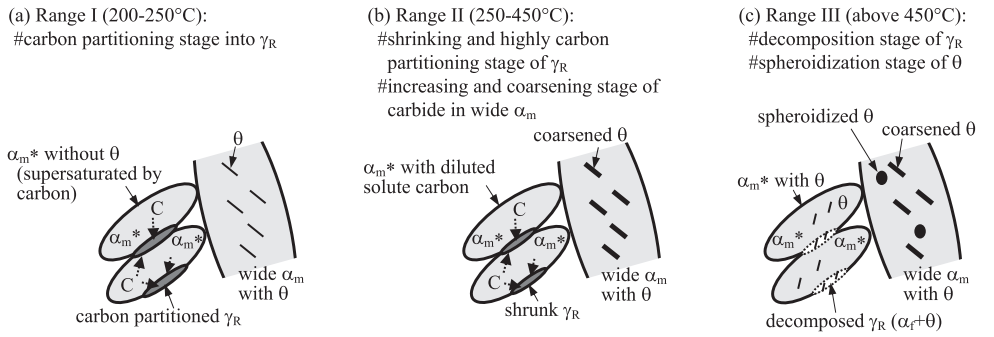

Fig. 12. Illustrations of microstructural change in wide and narrow lath martensite structure and retained austenite of TM steel partitioned at temperatures between Range I and Range III after quenching, in which α_m, α_m*, α_f, γ_R and θ represent wide lath martensite structure, narrow lath martensite structure, ferrite, retained austenite and carbide, respectively.

es: Range I, Range II, and Range III, as follows:

Range I (200–250°C): When the quenched TM steel is partitioned at temperatures lower than 250°C, the carbon concentration of the retained austenite increases considerably with increasing partitioning temperature (Fig. 10). Because the volume fractions of retained austenite and carbide are both constant (Fig. 10), supersaturated carbon in the martensite may move into the retained austenite (Fig. 12(a)).

Range II (250–450°C): When the steel is partitioned at temperatures higher than 300°C, the carbon concentration of the retained austenite increased to 1.0–1.1 mass%. The volume fraction of retained austenite decreases and the carbide content increases with increasing partitioning temperature (Fig. 10). Thus, it is thought that the retained austenite shrinks and the excess solute carbon causes the further precipitation or coarsening of the carbide (Fig. 12(b)).

Range III (above 450°C): When the steel is partitioned at temperatures above 450°C, most of the retained austenite phase decomposes into ferrite and carbide (Fig. 12(c)). In the wide martensite lath structure, spheroidal carbides coexist with coarsened needle-shaped carbides (Fig. 9(g)).

According to Nishiyama,[18] the decomposition of retained austenite into ferrite and cementite begins upon tempering at over 140°C in plain carbon steel. In this study, no retained austenite was decomposed into ferrite and carbide even in Range II. Therefore, we confirm that the retained austenite was shrunk in Range II.

Figure 13 shows a plot of the carbon concentration of the retained austenite of TM steel in an equilibrium diagram calculated for the C–1.5%Si–1.5%Mn system. The carbon concentrations at T_P = 350 and 400°C agree well with the T_0 line where austenite and ferrite with the same chemical composition have identical free energies.[19] However, the carbon concentration at 250°C is significantly lower than the T_0 line because of the low diffusion rate of carbon. From these results, it is expected that the upper limit of the carbon concentration of the retained austenite is the T_0 line, in the same way as for TBF steel.

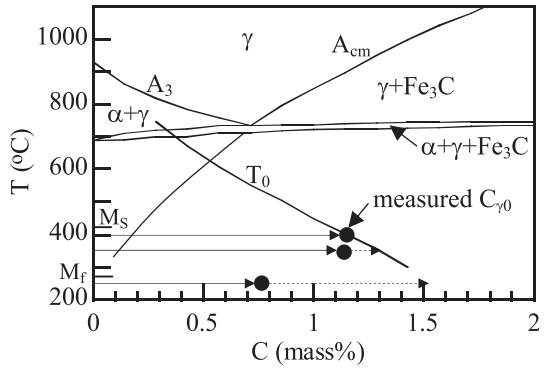

Fig. 13. Illustration of T_0 and A_{cm} temperatures in C–1.5%Si–1.5%Mn system, in which solid circle marks represent measured carbon concentration of retained austenite in TM steel quenched in oil.

5. Summary

The effects of partitioning after quenching in oil or ice-brine on the microstructure and retained austenite characteristics of 0.2%C–1.5%Si–1.5%Mn TM steel were investigated.

(1) The TM steel consisting of wide and narrow lath martensite structures contained retained austenite of about 3 vol% after quenching in oil, with carbides of 1.7–2.0 vol% only in the wider martensite lath structure. When the steel was quenched in ice-brine, the volume fraction of retained austenite decreased to 1.8 vol% with a decrease in the carbide volume fraction.

(2) With partitioning at temperatures lower than 250°C for times shorter than 1 000 s, the volume fractions of the retained austenite and carbide were maintained, although the carbon concentration of the retained austenite increased.

(3) On the other hand, partitioning at 300–400°C for 1 000 s after quenching caused a considerable increase in the carbon concentration of the retained austenite, although the volume fraction of retained austenite decreased and the volume fraction of carbide increased with increasing partitioning temperature.

Acknowledgment

This study was supported by the Grants from Adaptable and Seamless Technology Transfer Program through Target-driven R&D, the Japan Science and Technology Agency, and a Grant-in-Aid for Scientific Research (B), The Ministry of Education, Science, Sports and Culture, Japan (No.2008-20360311).

REFERENCES

1) B. C. De Cooman and J. G. Speer: *Steel Res. Int.*, **77** (2006), 634.
2) U. Brux, G. Frommeyer, O. Grassel, L. W. Meyer and A. Weise: *Steel Res.*, **73** (2002), 294.
3) K. Sugimoto, T. Iida, J. Sakaguchi and T. Kashima: *ISIJ Int.*, **40** (2000), 902.
4) K. Sugimoto, J. Sakaguchi, T. Iida and T. Kashima: *ISIJ Int.*, **40** (2000), 920.
5) K. Sugimoto, K. Nakano, S. Song and T. Kashima: *ISIJ Int.*, **42** (2002), 450.
6) K. Sugimoto, M. Tsunezawa, T. Hojo and S. Ikeda: *ISIJ Int.*, **44** (2004), 1608.
7) K. Sugimoto, M. Murata, T. Muramatsu and Y. Mukai: *ISIJ Int.*, **47** (2007), 1357.
8) K. Sugimoto, M. Murata and S. Song: *ISIJ Int.*, **50** (2010), 1357.
9) M. Murata, J. Kobayashi and K. Sugimoto: *Tetsu-to-Hagané*, **96** (2010), 84.
10) B. C. De Cooman: *Solid State Mater. Sci.*, **8** (2004), 285.
11) X. D. Wang, N. Zhong, Y. H. Rong, T. Y. Hsu (Z. Y. Xu) and L. Wang: *J. Mater. Res.*, **24** (2009), 260.
12) H. Maruyama: *J. Jpn. Soc. Heat Treat.*, **17** (1977), 198 (in Japanese).
13) D. J. Dyson and B. Holmes: *J. Iron Steel Inst.*, **208** (1970), 469.
14) O. Umezawa: *J. Jpn. Inst. Light Met.*, **50** (2000), 86.
15) D. Liu, B. Bai, H. Fang, W. Zhang, J. Gu and K. Chang: *Mater. Sci. Eng. A*, **371** (2004), 40.
16) D. P. Koistinen and R. E. Marburger: *Acta Metall.*, **7** (1959), 59.
17) J. Kobayashi, D. V. Pham and K. Sugimoto: *Steel Res. Int. 2011*, **Special Edition** (2011), 598.
18) Z. Nishiyama: Martensitic Transformation, applied ed., Maruzen Co., Tokyo, (1974), 114 (in Japanese).
19) M. Takahashi and H. K. D. H. Bhadeshia: *Mater. Trans.*, *JIM*, **32** (1991), 689.